

Performance of new crystal cathode pressure gauges for long-pulse operation in the Wendelstein 7-X stellarator

Uwe Wenzel,^{a)} Georg Schlisio, Matthias Mulsow, Thomas Sunn Pedersen, Martin Singer, Mirko Marquardt, Dirk Pilopp, and Nils Rüter

Max Planck Institute for Plasma Physics, Wendelsteinstrasse 1, 17491, Greifswald, Germany

To improve the reliability of the ASDEX pressure gauges in the plasma vessel of the Wendelstein 7-X stellarator, nine of them were equipped with a LaB₆ crystal electron emitter for the first time. These crystal cathode pressure gauges were operated during the last campaign in 2018 (operation phase 1.2b) with only 2 A heating current for over 40 h in a magnetic field of about 2.1 T without failure. Owing to this excellent performance, we have decided to equip all pressure gauges with crystal cathodes for the next campaign of Wendelstein 7-X (operation phase 2). We report on a pretest in a superconducting magnet, show a measurement of the neutral pressure in Wendelstein 7-X, and demonstrate the long-term stability of the crystal cathode pressure gauges.

^{a)}E-mail uwe.wenzel@ipp.mpg.de

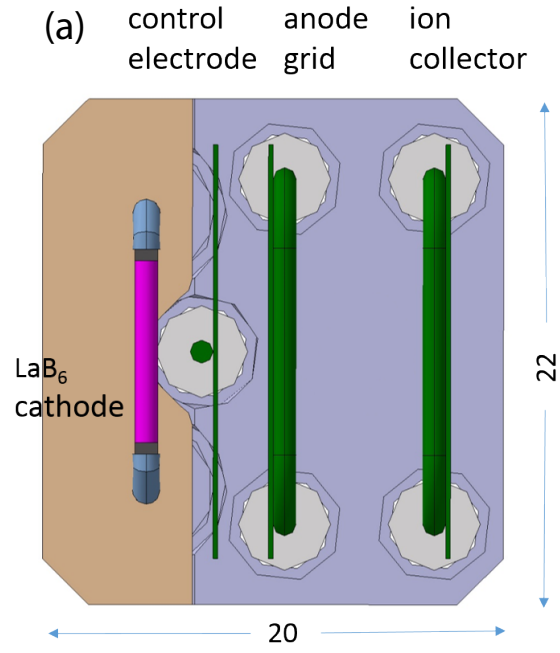
I. INTRODUCTION

Measurement of the neutral pressure is a key diagnostic for the island divertor of the Wendelstein 7-X stellarator. From the sub-divertor neutral pressure in front of the pumping ducts, it is possible to calculate the particle exhaust rate. ASDEX pressure gauges (APGs) are the state-of-the-art devices for these measurements in the strong magnetic fields of fusion devices.¹ They are used in several tokamaks, among them DIII-D² and ASDEX Upgrade,³ and their use is also foreseen for ITER.⁴ At ITER, they are called diagnostic pressure gauges (DPGs). We also use them in Wendelstein 7-X at several sub-divertor and midplane positions. The typical magnetic field is 2.1 T.

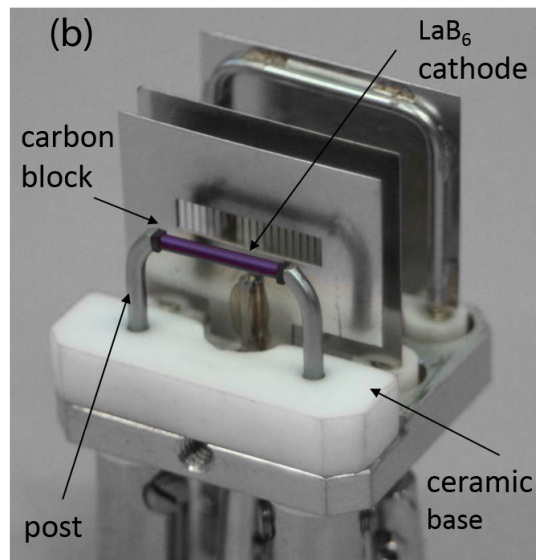
APGs are hot-cathode ionization pressure gauges. The first cathodes for Wendelstein 7-X were made from thoriated tungsten wires with a diameter of 0.6 mm (OSRAM G18). These cathodes were heated with currents between 14 and 18 A to obtain an electron current of 200 μA at the anode grid. However, in the first two operation phases, namely, OP1 and OP1.2a, they were frequently found to be deformed, presumably as a result of the $\mathbf{j} \times \mathbf{B}$ force on the cathode wires.⁵ Since we use plug-ins to position the pressure gauges, we were able to retract them to repair the damaged ones. This could be done only between operation phases, so not all installed APGs were available for pressure measurements.

Similar problems were reported from the tokamaks JET⁶ and KSTAR.⁷ As in Wendelstein 7-X, the typical bending pattern of a 0.6 mm tungsten wire can lead to a short circuit by a contact with the control electrode.

Hoping to improve the robustness of the pressure gauges, we substituted the tungsten wires with a different emitter for 11 of the APGs during the third operation phase of Wendelstein 7-X, OP1.2b. This type of pressure gauge was recently developed by Wenzel *et al.*⁸ It makes use of a LaB_6 crystal rod as a thermionic bulk emitter. LaB_6 has the advantage of better electron emission than thoriated tungsten by the lower work function. With the LaB_6 crystal, the pressure gauge was operated in the laboratory with a very low heating current of 1.5 A, i.e., with a considerably lower current than needed for the APGs with the 0.6 mm tungsten cathodes.



(a)



(b)

FIG. 1. (a) Schematic of the pressure gauge head with the LaB₆ cathode (birds eye view) and (b) the realized gauge head mounted in the port AEP51.

The successful initial test in a superconducting magnet at comparable field strength and

hydrogen pressures (see Sec. II) encouraged us to use a larger number in Wendelstein 7-X. After OP1.2a, 8 pressure gauges either remained unchanged or were equipped with a fresh tungsten cathode, while the other 11 were replaced by the new pressure gauges. We call the new design a crystal cathode pressure gauge (CCPG). These are basically ASDEX pressure gauges with a crystal emitter, although the crystal emitter is not the only distinguishing feature: in addition, the distance between the emitter and the control electrode, as well as the electrode biasing settings, are different from previous gauges. Crystals cannot be Ohmically heated because of the low resistance. Instead, small pyrolytic graphite blocks are heated by Ohmic dissipation, and the blocks, in close contact with the crystal, heat the crystal indirectly (the so-called Vogel mount;⁹ see also Fig. 1 for an image of the crystal emitter).

We report on the performance of the CCPGs in Wendelstein 7-X during OP1.2b. First, some results of a pretest in a superconducting magnet are described in Sec. II. In Sec. III, the set-up of the 11 CCPGs in Wendelstein 7-X is described. Two of the CCPGs had some problems from the beginning. One was not functional after baking, while the other was not exactly oriented along the magnetic field, with the consequence that only a small electron current could be drawn from the LaB₆ emitter. Neither pressure gauge was routinely operated. The calibration of the nine other CCPGs is also described in Sec. III. In Sec. IV, we report on the behavior of the CCPGs in OP1.2b. We give an example of a neutral pressure measurement and demonstrate the large reduction of the heating current of the CCPG in a direct comparison with a standard APG. Finally, we characterize the long-term behavior of the CCPGs in Sec. V from three different aspects: stability of the heating current in a strong magnetic field, stability of the pressure measurement, and visual inspection after OP1.2b.

II. PRETESTS IN A SUPERCONDUCTING MAGNET

Before the application in Wendelstein 7-X, we tested the first prototype of a CCPG over 5 days in a superconducting magnet at 3.1 T. Details of the pressure gauge with LaB₆ crystal emitter and the experimental set-up are described in Ref. 8. The long-term test was carried out in the following way. The pressure was set to 5×10^{-3} mbar hydrogen using a Baratron mounted 1 m away from the magnet. The pressure on the axis of the magnet (at 3.1 T) was measured continuously over 29 min with the CCPG. After a break of 1 min, the next measurement, with a sample time of 29 min, was started. This procedure was repeated

for 12 h per day. We performed in total $24 \times 5 = 120$ measurements and accumulated $29 \text{ min} \times 120 = 58 \text{ h}$ operation time.

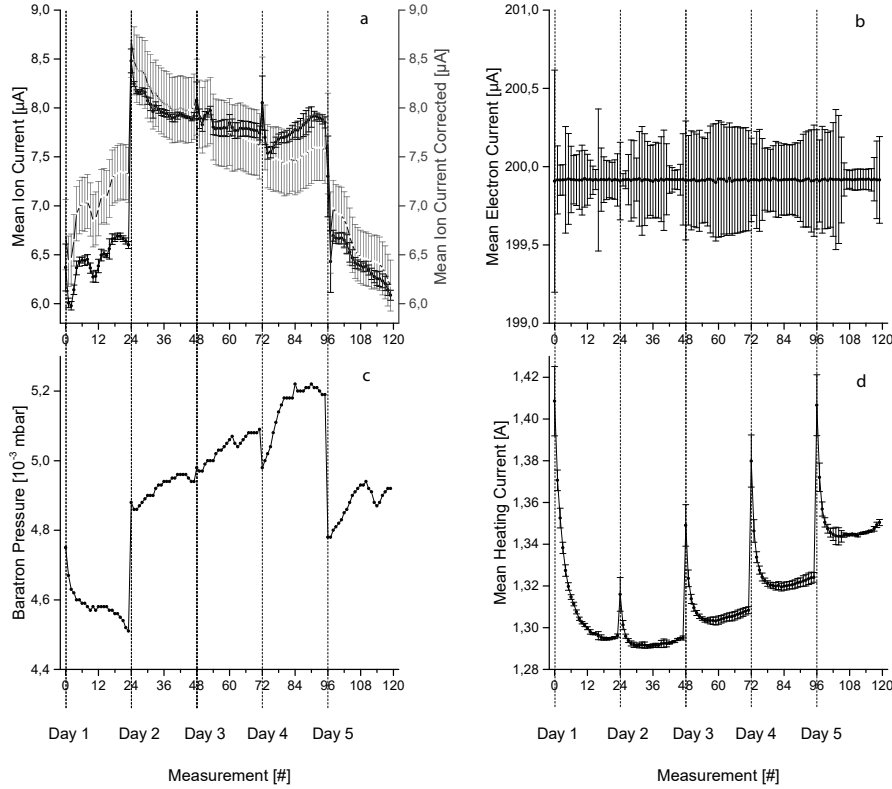


FIG. 2. Response of the CCPG in a steady-state magnetic field of 3.1 T over 58 h. The reference pressure was measured with a Baratron. It is about 5×10^{-3} mbar [see (c)]. The CCPG data (raw ion (a, black line), electron (b), and heating current (d)) are plotted vs the number of the measurement. The ion current of the CCPG was normalized to the reference pressure (gray line in (a)).

During the long-time experiment, the CCPG was operated in feedback mode on an electron current of $200 \mu\text{A}$. Figure 2 shows the ion and heating currents in each of the measurements and the hydrogen pressure as measured by the Baratron. Since we did not actively control the pressure, it varied over the five experimental days. To eliminate this variation, the measured ion current was normalized to the pressure measured with the Baratron. The CCPG data were averaged over 25 min, with the exception of the first 5 min.

The heating current shows two characteristic effects. At the start of each day, a decrease is observed. We call this the *formation effect*, and it occurs after a rest of 12 h in vacuum

without hydrogen gas. By fitting the decaying current level to an exponential function, a formation time of 42 min is obtained. We suspect that this is due to the capability of the carbon blocks to store hydrogen (see the discussion in Sec. V A). Another effect is the small increase in the heating current from day to day. We call this the *aging effect*. Assuming a linear aging trend, the heating current limit of 3 A (to avoid overheating of the emitter unit) would be reached after 1172 h.

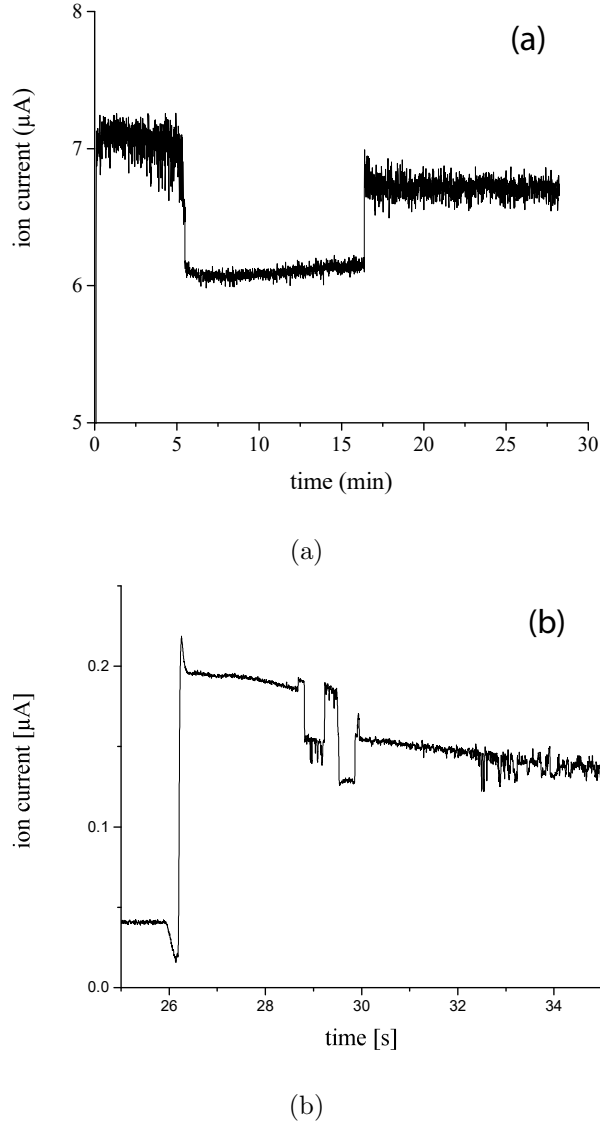


FIG. 3. Spontaneous jumps of the ion currents of different pressure gauges at (nearly) constant hydrogen pressure: (a) LaB₆ cathode (superconducting magnet); (b) tungsten cathode (Wendelstein 7-X). This instability limits the measurement accuracy. When we take the jumps observed in the ion current of the CCPG, the accuracy is estimated to be 15%.

We observed that the ion current is not constant as expected for a constant hydrogen pressure [see Fig. 2(a)]. We think that this is the consequence of an ambiguity of the ion current, because the ion current exhibited sometimes spontaneous jumps during the 29 min runs in the magnet. Figure 3(a) shows examples of jumps observed during the long-term experiment and in Wendelstein 7-X. In the CCPG, spontaneous jumps of the ion current occurred despite a constant hydrogen pressure. In this particular example, the ion current jumped from 7.1 to 6.1 μA and stayed at this level for more than 10 min. Then a jump to 6.7 μA occurred and, again, the ion current stayed at this level for more than 10 min. It must be emphasized that the electron current was constant at 200 μA for all three levels of ion current due to the feedback operation. Such behavior is not a property of the LaB_6 cathode, but was also observed in pressure gauges with cathodes made from tungsten wires [see the example in Fig. 3(b) from Wendelstein 7-X]. The electron current had the same value of 200 μA . We see a transition between two levels with an ambiguous behavior in the transition phase. The measurement accuracy is reduced by this instability, since we do not know which level the pressure gauge is in during the measurement compared with the level during the calibration. When we take the jump from 7.1 μA to 6.1 μA , i.e., 1 μA (which is about 15% from the larger value of 7.1 μA), then the accuracy is about 15%. The example from Wendelstein 7-X shows even larger relative jumps of about 25%, but this seems to be the case only in a transition phase from level 1 to level 2. At the moment we have no sure explanation for this effect.

Finally, we studied the behavior of the CCPG at high neutral pressures. In hydrogen, we found an upper pressure limit of 2×10^{-2} mbar. At this pressure, the ion current begins to saturate. Since for the island divertor of Wendelstein 7-X, maximum values of the order of 10^{-3} mbar were predicted,¹⁰ this limit is sufficient for the experiments in Wendelstein 7-X.

III. SET-UP AND CALIBRATION OF THE CCPGs

The successful pretest of the CCPG in the superconducting magnet encouraged us to install 11 CCPGs in Wendelstein 7-X. After baking and the first tests, we found nine of them to be fully functional, while two had severe problems that prevented operation. These problems, however, were not caused by the pressure gauges themselves but by the mounting. Table I shows some details of the set-up of the remaining nine CCPGs.

TABLE I. Details of the spatial positions and the calibration factors C of the nine CCPGs in Wendelstein 7-X. Calibration of the CCPG in port AEH41 was obtained after the operation phase 1.2b (C is marked by an asterisk).

Port used	Functionality	Module	Position	$C / 10^{-4}$ mbar/ μ A
AEA21	Plasma vessel	2	Midplane	2.845
AEH30	Pumping duct (standard)	3	Bottom	4.0627
AEP30	Pumping duct (high iota)	3	Bottom	3.892
AEE41	Plasma vessel	4	Midplane	2.2146
AEP51	Pumping duct (high iota)	5	Top	2.5248
AEH41	Pumping duct (standard)	4	Top	2.5835*
AEI30	Pumping gap (standard)	4	Bottom	2.7546
AEI50	Pumping gap (standard)	5	Bottom	2.6260
AEI51	Pumping gap (standard)	5 <td Top	2.5846	

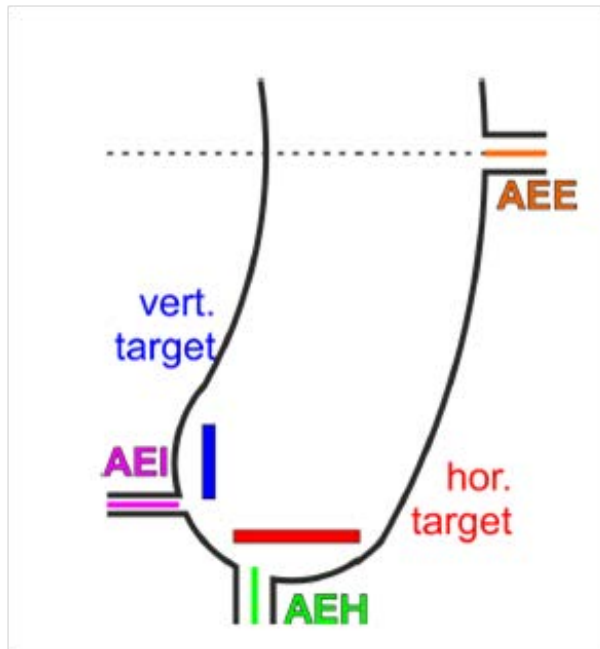


FIG. 4. Schematic poloidal cross section of Wendelstein 7-X with some typical positions of the CCPGs: near the divertor pumping gap (port AEI), in the pumping duct (port AEH) and midplane (ports AEE and AEA).

The CCPGs were positioned at several relevant positions in the plasma vessel: two in midplane positions, three near the pumping gaps of the divertor (through port AEI), and four in the front of the pumping ducts (two in the AEP ducts and two in the AEH ducts). Figure 4 shows a poloidal cross section of W7-X with the positions of the CCPGs. The highest pressures were expected near the pumping gaps of the island divertor (port AEI) and the lowest at the midplane (port AEE or AEA). The placement of gauges at different positions ensures that the CCPGs are tested over a wide pressure range.

At the beginning of the campaign all CCPGs were calibrated against a reference pressure obtained from gas type independent capacitance manometers and gas type corrected Penning gauges in their respective pressure range. The calibration was performed in magnetic standard configuration as was set up as a series of hydrogen puffs into an unpumped vacuum vessel leading to phases of equilibrated pressure. The obtained ion current was fitted to the reference pressure with a linear model without offset ($p = C * I_i$), which is a common approach for hot ion cathode gauges in the low and medium pressure range (see also Figure 9). Figure 5 shows the time traces of the calibrated CCPGs overplotted with the reference pressure. Residual deviations could be corrected with a more complex model. All calibrations were only performed for an electron current of 200 μA , at which all CCPGs were operated throughout the campaign.

All calibration factors are listed in Table I. The mean calibration factor over 8 gauges is $C = 2.9 \times 10^{-4} \text{ mbar}/\mu\text{A}$. The mean sensitivity, defined as

$$S = \frac{I_i}{I_e * p} = \frac{1}{I_e * C}$$

is calculated to be $S = 17 \text{ mbar}^{-1}$. This value is about twice as large as that found in the laboratory experiments for $I_e = 200 \mu\text{A}$ (7 mbar^{-1} , see Figure 6 in⁸).

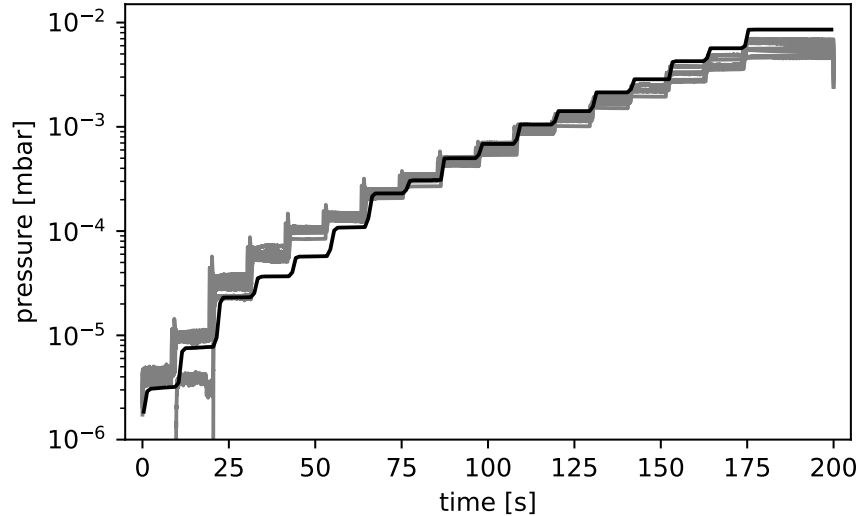


FIG. 5. Pressure steps in hydrogen gas in the vacuum vessel of Wendelstein 7-X with standard magnetic field. The reference pressure is plotted in black. All CCPGs are plotted in gray with their individual calibration factors given in Table I.

IV. MEASUREMENT RESULTS

During OP1.2b, the CCPGs were operated for a total of about 40 h in the magnetic field, i.e., slightly less than in the long-term test in the magnet. We start the analysis of the performance of the CCPGs with an example of the pressure measurements in the standard divertor configuration. Then we compare the heating current of the new LaB₆ cathode design with that of the standard APG with a tungsten cathode.

A. Example of a neutral pressure measurement

Figure 6 shows the pressure distribution of a typical plasma experiment in the so-called standard divertor configuration. In this configuration, particles are mainly deposited at the low-iota tail of the divertor target (near the AEH and AEI ports). This experiment has three electron cyclotron resonance heating (ECRH) power steps (2 MW, 3 MW, and 4 MW) at an almost constant line-integrated density of $5 \times 10^{19} \text{ m}^{-2}$. Figure 6 shows the neutral pressures measured in the midplane (an average of AEE41 and AEA21), in the pumping ducts (AEH41 and AEH30), and near the pumping gaps (AEI50 and AEI51).

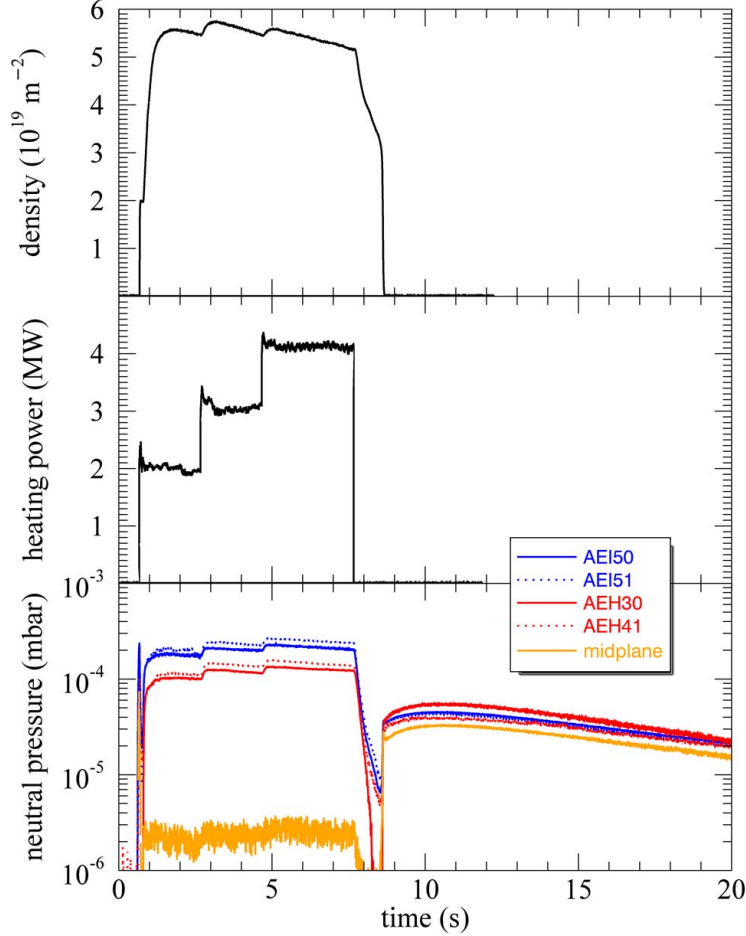


FIG. 6. Neutral pressures in a typical plasma experiment with three heating power steps and constant plasma density (in the so-called magnetic standard configuration). The experiment number is 20181010.005.

We can distinguish two phases. The *experiment phase* is 7 s long and is followed by the *outgassing phase*. In the experiment phase, the three power steps are clearly visible in the sub-divertor neutral pressures. The maximum pressure is measured near the pumping gap. The sub-divertor pressure at the pumping ducts is a factor of 2 lower. The neutral compression, defined as the pressure ratio between midplane and pumping duct (AEH), is about 50. The sub-divertor neutral pressures in the divertors on top are slightly higher. In the outgassing phase, there is no plasma and no gas fueling from external valves. Neutral particles that are released from the first wall fill the plasma vessel, and the measured neutral pressures are close to each other, independently of the position of the pressure gauge.

The maximum sub-divertor neutral pressure was 2×10^{-3} mbar measured in the AEP51

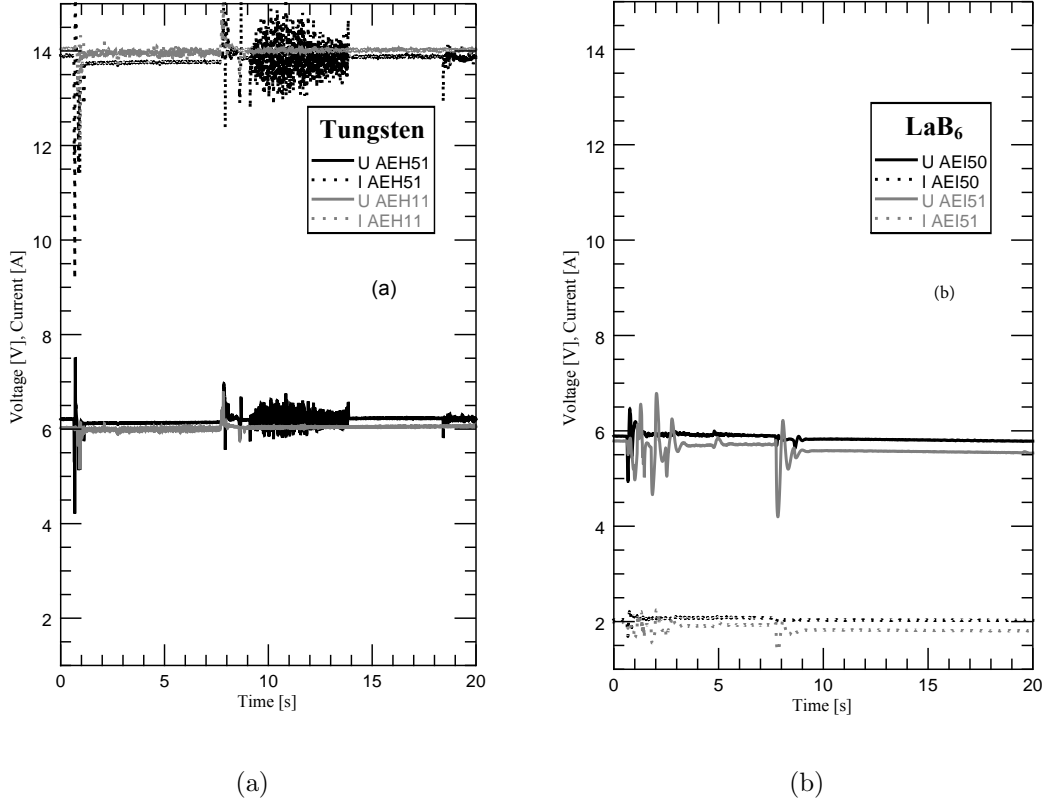


FIG. 7. Comparison of the heating currents I and voltages U of the two types of pressure gauge in the same experiment as shown in Fig. 6: (a) with tungsten cathodes; (b) with LaB_6 cathodes. With the new LaB_6 cathode design, the heating current is reduced from 14 A to 2 A.

pumping duct in the magnetic high-iota configuration.

B. Comparison of the heating currents of APG and CCPG

The new pressure gauges were designed to reduce the heating current of the emitter in the magnetic field. Figure 7 compares the electrical parameters of the cathode circuits of both types of pressure gauge. Data were sampled in the experiment 20181010.005 shown in Fig. 6. The time interval in Fig. 7 is the same as in Fig. 6. APG data are from two AEH pumping duct positions (AEH11 in module 1 and AEH51 in module 5). The electron current at the anode grid was set to 200 μA , independently of pressure gauge type. CCPGs need about 2 A to obtain this current, while the heating current for the two APGs is 14 A. The voltage of the power supply needed to drive the heating currents is about 6 V in both cases.

V. LONG-TERM BEHAVIOR OF THE CCPGs IN WENDELSTEIN-X

A. Heating current of the LaB₆ emitter

All nine CCPGs were operated for 40 h in the magnetic field of Wendelstein 7-X without failure, i.e., a bit less than the long-term test in the superconducting magnet. Figure 8 shows the current and resistance of an emitter circuit from all experiments in OP1.2b. Data are from the pressure gauge in port AEA21 (midplane position in the plasma vessel, module 2). The pressure measurement was started 20 s before the ignition of the plasma. Data are averaged between 6 and 19 s after the trigger event, i.e., in the time before the plasma.

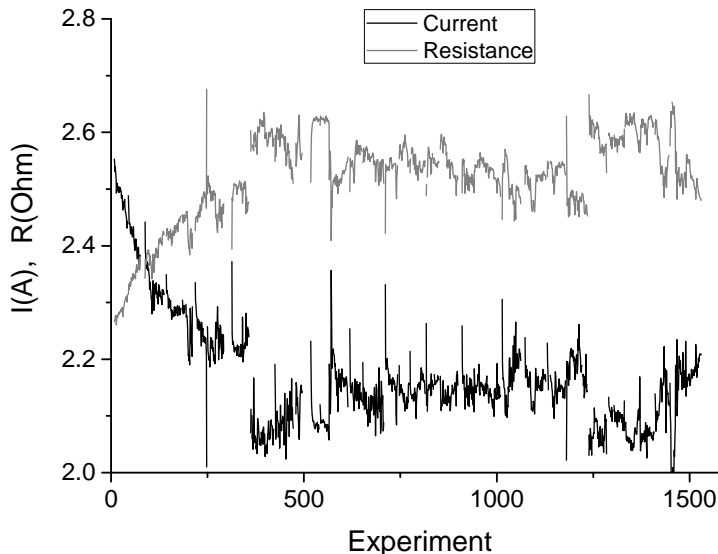


FIG. 8. Heating current I and resistance R of the emitter circuit of the CCPG in port AEA21 vs experiment number. Data are from the whole of OP1.2b. The heating current is feedback-controlled to ensure an electron current of $200 \mu\text{A}$ at the anode grid.

The resistance increases in the first 250 experiments from 2.3Ω to 2.5Ω . In the same time, the heating current decreases from 2.5 A to about 2.25 A . Furthermore, two sudden jumps are observed in the resistance from 2.5Ω to 2.6Ω and consequently in the heating current, too.

We interpret the data as follows. The resistance of the emitter circuit is determined by the carbon blocks, which are the elements with the highest resistance compared with the

posts and to the crystal. The change in resistance is consequently due to the carbon blocks. Carbon is known for its property of storing a substantial amount of hydrogen. In the initial phase, the blocks store hydrogen, which presumably increases their electrical resistance. This hypothesis is supported by laboratory studies. At least for raw graphite, an increase in resistance was found when hydrogen was stored.¹¹ By this effect, the blocks become hotter and less heating current is needed to obtain an electron current of 200 μA at the anode grid. After 250 experiments, the blocks are saturated with hydrogen, and the resistance stays constant. The two jumps in resistance from 2.5 Ω to 2.6 Ω correlate with the boronization of the plasma vessel. Apparently, the boronization can also change the resistance of the blocks. Again, the higher resistance leads to a lower heating current owing to the hotter blocks.

The absolute current limit of the LaB₆ emitters is 4 A. It is determined by the maximum allowed temperature of the carbon blocks. With the heating current in the range of 2.1–2.5 A before plasma operation, there is a sufficient margin to the 4 A limit of the emitters during the plasma phase.

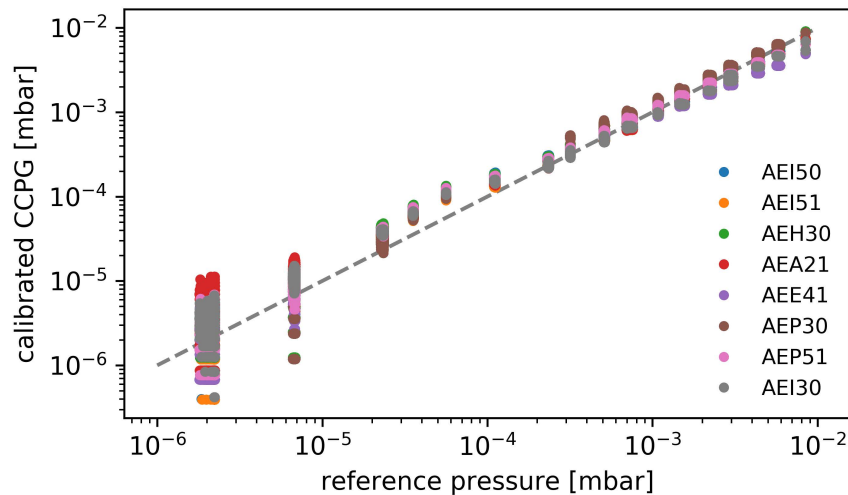


FIG. 9. Comparison of reference pressure and calibrated CCPG sensor data overplotted with the dashed line of ideal match. For the CCPGs the calibration from beginning of the campaign was used, signal and reference pressure were measured at the end of the campaign. All CCPGs still work and show no significant sensor drift.

B. Long-term stability of the pressure measurement

To check the long-term stability of the pressure gauges, the calibration was repeated at the end of OP1.2b. Again, a pressure ramp was carried out with hydrogen gas inlet into the plasma vessel with closed gate valves only, i.e. without plasma. The magnetic field was set to the standard configuration. Figure 9 shows the result of the procedure using the individual calibration factors determined at the beginning of OP1.2b (see Table I). All pressure gauges measure the pressure steps within a certain interval; above 10^{-5} mbar there is no pressure gauge with a larger deviation than the estimated 15% accuracy. All pressure gauges were fully functional after 40 h operation in the magnetic field. Only one CCPG in port AEP51 had a temporary problem: the heating current showed some low frequency oscillations, but these disappeared after a while.

C. Visual inspection of the CCPGs after operation

After OP1.2b, all CCPGs were removed. The pressure gauge heads were dismantled from the plug-ins and stored in a desiccator. We found no degradation of the emitter units. The gauge head from port AEP51 may serve as an example (Fig. 1). This position was selected because it was there that we measured the highest neutral pressures. Only a thin layer is visible on the control electrode, but it does not affect operation. Such a layer was expected because some cathode material is evaporated during operation. This result suggests that all emitters can be used again in the next operation phase, in contrast to the APGs. Some tungsten cathodes were heavily deformed in the magnetic field and could not be operated over the whole of OP1.2b. An example of such a deformation is given in Ref. 5.

VI. CONCLUSION

The CCPGs exhibited a very good performance in Wendelstein 7-X during OP1.2b. We demonstrated the operation of nine pressure gauges over 40 h in a magnetic field of about 2.1 T without failure. We believe that the stable behavior of the CCPGs is due to the strong reduction in heating current. Data were used to characterize particle exhaust and neutral compression in the island divertor with an accuracy of 15%. The robust design we hoped to achieve was confirmed: the LaB_6 emitter had no problems with boronization of the vacuum

vessel, gas injection into the vacuum vessel for radiation cooling, or the hydrogen gas at high neutral pressures.

The next campaign, operation phase 2 (OP2), is planned with an actively cooled island divertor for long-pulse operation. Because of the persistent problems with the APGs (with thoriated tungsten cathodes), we have decided to equip Wendelstein 7-X only with CCPGs for the future. A full setup with 18 CCPGs will allow a more comprehensive testing of this new concept during long-pulse plasma operation and, hopefully, over longer operation times in a magnetic field.

ACKNOWLEDGMENTS

We would like to thank B. Magera and B. Mackie from AP-TECH for supplying the LaB₆ cathodes. A. Scarabosio wrote the software for testing the CCPG prototype in the superconducting magnet. We also thank A. Graband for excellent technical support.

This work has been carried out within the framework of the EUROfusion Consortium and has received funding from the Euratom Research and Training Programme 2014-2018 and 2019-2020 under grant agreement No 633053. The views and opinions expressed herein do not necessarily reflect those of the European Commission.

REFERENCES

- ¹G. Haas and H.-S. Bosch. In vessel pressure measurement in nuclear fusion experiments with ASDEX gauges. *Vacuum*, 51:39–46, 1998.
- ²C. C. Klepper, T. E. Evans, G. Haas, G. L. Jackson, and R. Maingi. Neutral pressure studies with a fast ionization gauge in the divertor region of the DIII-D tokamak. *Journal of Vacuum Science & Technology A: Vacuum, Surfaces, and Films*, 11(2):446–450, 1993.
- ³A. Scarabosio, G. Haas, H. W. Müller, R. Pugno, and M. Wischmeier. Measurements of neutral gas fluxes under different plasma and divertor regimes in ASDEX Upgrade. *Journal of Nuclear Materials*, 390-391(Supplement C):494 – 497, 2009. Proceedings of the 18th International Conference on Plasma-Surface Interactions in Controlled Fusion Devices.
- ⁴A. Arkhipov, A. Scarabosio, G. Haas, F. Mackel, J. Koll, H. Meister, H. Eixenberger,

- O. Paz, F. Seyvet, S. Terron, and P. Andrew. Status of the development of diagnostic pressure gauges for the operation in ITER. *Fusion Engineering and Design*, 12 2016.
- ⁵U. Wenzel, T. Kremeyer, G. Schlisio, M. Marquardt, T.S. Pedersen, O. Schmitz, B. Mackie, J. Maisano-Brown, and the W7-X team. Advanced neutral gas diagnostics for magnetic confinement devices. *Journal of Instrumentation*, 12(09):C09008, 2017.
- ⁶G. Haas, R. E. Wirth, H. J. Albrecht, J. Ehrenberg, T. Schneider, and H. Völkel. Tests of Pressure Gauges in High-Magnetic Fields at Forschungszentrum Karlsruhe (FZK). Technical Report IPP 2019-14, Max-Planck-Institut für Plasmaphysik, Garching, Germany, 2019. <http://hdl.handle.net/21.11116/0000-0003-F279-4>.
- ⁷M. Kim, K. Kim, and H. Lee. The new attempts for the in-vessel pressure gauge operation in the KSTAR plasma. *Fusion Engineering and Design*, 146:2011–2014, 2019.
- ⁸U. Wenzel, T. S. Pedersen, M. Marquardt, and M. Singer. An ionization pressure gauge with LaB₆ emitter for long-term operation in strong magnetic fields. *Review of Scientific Instruments*, 89(3):033503, 2018.
- ⁹S. F. Vogel. Pyrolytic graphite in the design of a compact inert heater of a lanthanum hexaboride cathode. *Review of Scientific Instruments*, 41(4):585–587, 1970.
- ¹⁰Y. Feng, F. Sardei, P. Grigull, K. McCormick, J. Kisslinger, and D. Reiter. Physics of island divertors as highlighted by the example of W7-AS. *Nucl. Fusion*, 46:807–819, 2006.
- ¹¹J. Im, S. Yang, and Y. Lee. Investigation of the hydrogen storage mechanism of expanded graphite by measuring electrical resistance changes. *Bulletin of the Korean Chemical Society*, 9:3033–3038, 2012.